

## CONTROLLING PEM FUEL CELLS APPLYING A CONSTANT HUMIDITY TECHNIQUE

### **Luis A.M. Riascos**

Federal University of ABC  
r. Santa Adelia, 166, Santo Andre – SP, Brazil  
luis.riascos@ufabc.edu.br

### **Marcelo G. Simoes**

Colorado School of Mines  
1500 Illinois St, Golden – CO, USA  
mgs@mines.edu

### **Paulo E. Miyagi**

University of Sao Paulo  
Av. Prof. Mello Moraes, 2231, Sao Paulo – SP, Brazil  
pemiagi@usp.br

**Abstract.** Proton exchange membrane fuel cells (PEMFCs) have attracted great attention in recent years as a promising replacement for traditional stationary and mobile power sources, especially due to their high power density and low greenhouse gas emissions. However, a number of fundamental problems must be overcome to improve their performance and to reduce their cost. A control system is needed to ensure that the airflow rate and temperature are within prescribed limits during operation. The water content on the membrane influences the fuel cell (FC) performance, and this can be controlled by relative humidity. Therefore, in this research, a new control technique based on the regulation of relative humidity is introduced. The ideal operational condition is relative humidity in saturated conditions; the proposed control system adjusts the air-reaction volume to maintain this condition.

From the mathematical model developed in Matlab<sup>®</sup>, the evolutions of some variables that can be difficult to monitor in a real machine are observed. Also, prediction about the evolution of variables can be tested, optimizing time and resources. For experimental validation, tests in a fault tolerant fuel cell (FTFC) are conducted.

**Keywords:** Proton exchange membrane fuel cells, control systems, relative humidity control, computer simulation.

## 1. INTRODUCTION

Major efforts to reduce greenhouse gas emission have increased the demand for pollution-free energy sources. Fuel cell (FC) has attracted great attention in recent years as a promising replacement for traditional stationary and mobile power sources, especially due to their high power density and low greenhouse gas emissions.

FC is an electrochemical device that generates electricity, similar to batteries, but which can be continuously fueled. Under certain pressure, hydrogen ( $H_2$ ) is supplied into a porous conductive electrode (the anode).  $H_2$  spreads through the electrode until it reaches the catalytic layer of the anode, where it reacts, separating protons and electrons. The  $H^+$  protons flow through the electrolyte (a solid membrane), and the electrons pass through an external electrical circuit, producing electrical energy. On the other side of the FC, oxygen ( $O_2$ ) spreads through the cathode and reaches its catalytic layer. On this layer,  $O_2$ ,  $H^+$  protons, and electrons produce liquid water and residual heat as sub-products (Larminie and Dicks, 2003).

Significant improvements in proton exchange membrane fuel cell (PEMFC) technology have been achieved over the past decade. However, the performance, stability, reliability, and cost for the present FC technology are not enough to replace internal combustion engines. A number of fundamental problems must be overcome to improve their performance and reduce their cost.

The control, design, and optimum operation of FC require an understanding of the dynamics when there are changes in electrical current, voltage, or power. A control system is needed to ensure that the flow rate and temperature of fuel and air are within prescribed limits during normal operation at variable loads, as well as during system start-up and shut-down.

The FC performance is influenced by the water content on the membrane; that can be controlled through the relative humidity inside the FC. Therefore, this research introduces a new control technique based on the regulation of the relative humidity.

This paper is organized as follows. In section 2, the basic concepts for the mathematical model of a PEMFC are introduced. Section 3 introduces the proposed control technique and presents simulation tests. Section 4 presents tests for experimental validations and description of the experimental equipment. In section 5, main conclusions are reported.

## 2. THE FUEL CELL MODEL

Many mathematical models of PEMFC can be found in the literature (Correa et al., 2004), (Fouquet et al., 2006), and (Promislow and Wetton, 2005). Basically, a model of PEMFC consists of an electro-chemical and thermo-dynamical sub-models. Correa et al. (2004) introduce an electro-chemical model of a PEMFC; to validate the model, the polarization curve obtained with this model is compared to the polarization curve of the manufacturing data sheet. In (Riascos et al., 2007), the thermo-dynamical part of the model is included to study the effects of different types of faults.

### 2.1. The Electrochemical Model

The output voltage  $V_{FC}$  of a single cell can be defined as the result of the following expression (Larminie and Dicks, 2003):

$$V_{FC} = E_{Nernst} - V_{act} - V_{ohmic} - V_{con} \quad (1)$$

$E_{Nernst}$  is the thermodynamic potential of the cell representing its reversible voltage:

$$E_{Nernst} = 1,229 - 0,85 \cdot 10^{-3} \cdot (T - 298,15) + 4,31 \cdot 10^{-5} \cdot T \cdot \left[ \ln(P_{H_2}) + \frac{1}{2} \cdot \ln(P_{O_2}) \right] \quad (2)$$

where:  $P_{H_2}$  and  $P_{O_2}$  (atm) are the hydrogen and oxygen pressures, respectively, and  $T$  (K) is the operating temperature.

$V_{act}$  is the voltage drop due to the activation of the anode and the cathode:

$$V_{act} = -\left[ \xi_1 + \xi_2 \cdot T + \xi_3 \cdot T \cdot \ln(c_{O_2}) + \xi_4 \cdot T \cdot \ln(I_{FC}) \right] \quad (3)$$

where:  $\xi_i$  ( $i = 1 \dots 4$ ) are specific coefficients for every type of FC,  $I_{FC}$  (A) is the electrical current, and  $c_{O_2}$  is the oxygen concentration.

$V_{ohmic}$  is the ohmic voltage drop associated with the conduction of protons through the solid electrolyte, and electrons through the internal electronic resistance:

$$V_{ohmic} = I_{FC} \cdot (R_M + R_C) \quad (4)$$

where:  $R_C$  ( $\Omega$ ) is the contact resistance to electron flow, and  $R_M$  ( $\Omega$ ) is the resistance to proton transfer through the membrane:

$$R_M = \frac{\rho_M \cdot \ell}{A}, \quad \rho_M = \frac{181,6 \cdot \left[ 1 + 0,03 \cdot \left( \frac{I_{FC}}{A} \right) + 0,062 \cdot \left( \frac{T}{303} \right)^2 \cdot \left( \frac{I_{FC}}{A} \right)^{2,5} \right]}{\left[ \psi - 0,634 - 3 \cdot \left( \frac{I_{FC}}{A} \right) \right] \cdot \exp \left[ 4,18 \cdot \left( \frac{T - 303}{T} \right) \right]} \quad (5)$$

where:  $\rho_M$  ( $\Omega \cdot \text{cm}$ ) is the membrane specific resistivity,  $\ell$  (cm) is the membrane thickness,  $A$  ( $\text{cm}^2$ ) is the membrane active area, and  $\psi$  is a specific coefficient for every type of membrane.

$V_{con}$  represents the voltage drop resulting from the mass transportation effects, which affects the concentration of the reacting gases:

$$V_{con} = -B \cdot \ln \left( 1 - \frac{J}{J_{max}} \right) \quad (6)$$

where:  $B$  (V) is a constant depending on the type of FC,  $J_{max}$  is the maximum electrical current density, and  $J$  is the electrical current density produced by FC. In general,  $J = J_{out} + J_n$  where  $J_{out}$  is the real electrical output current density, and  $J_n$  represents the fuel crossover and internal current loss.

Considering a stack composed by several FCs, the output voltage can be assumed to be  $V_S = nr \cdot V_{FC}$ , where  $nr$  is the number of cells composing the stack. However, constructive characteristics of the stack, such as flow distribution and heat transfer, could influence the output voltage of each cell (Chang et al., 2006), (Freunberger et al., 2006), (Kim et al., 2005) and (Santis et al., 2006).

### 2.2. The Thermo-Dynamical Model

The calculation of the relative humidity and the operating temperature of the FC essentially compose the thermo-dynamical model.

### 2.2.1. Temperature

The variation of temperature in the FC is obtained with the following differential equation:

$$\frac{dT}{dt} = \frac{\Delta\dot{Q}}{M \cdot C_s} \quad (7)$$

where:  $M$  (kg) is the whole stack mass;  $C_s$  (J/K·kg) is the average specific heat coefficient of the stack; and  $\Delta\dot{Q}$  is the rate of heat variation (i.e., the difference between the rate of heat generated by the cell operation and the rate of heat removed). Four types of heat removed are considered: heat by the reaction air flowing in the stack ( $Q_{rem1}$ ), by the refrigeration system ( $Q_{rem2}$ ), by water evaporation ( $Q_{rem3}$ ), and by heat exchanged with the surroundings ( $Q_{rem4}$ ).

The rate of heat generated in a FC is calculated from the following equation (Larminie and Dicks, 2003):

$$\dot{Q}_{ger} = Pow_s \cdot \left( \frac{1,48}{V_{FC}} - 1 \right) \quad (8)$$

where:  $Pow_s$  is the power produced by the stack

### 2.2.2. Relative Humidity

A correct humidity level should be maintained in the FC. This level is measured through the relative humidity.

If the relative humidity is much smaller than 100%, then the membrane dries out and the conductivity decreases. On the other hand, a relative humidity greater than 100% produces accumulation of liquid water on the electrodes, which can become flooded and block the pores, making gas diffusion difficult. The result of these two conditions is a fairly narrow range of normal operating conditions.

In (Bao et al., 2006), the water and thermal management in fuel cell systems were analyzed considering humidification at the cathode and anode. Forms of humidification can include liquid water injection, direct membrane humidification, recycling-humidification and many other methods; in (Zhan et al., 2006), the parameters that affect the liquid water flux through the membrane and gas diffusion layer are analyzed.

Figure 1 associates the variation of temperature and relative humidity for different air stoichiometric ratios ( $\lambda=2$ ,  $\lambda=4$  e  $\lambda=8$ ). The stoichiometry  $\lambda$  is the relationship between inlet air divided by the air necessary for the chemical reaction.

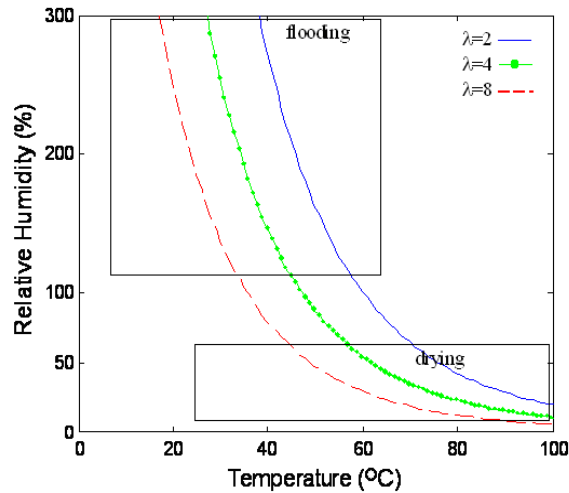


Figure 1. Temperature and relative humidity for  $\lambda=2,4,8$ .

Figure 2 illustrates the effects on the performance of a FC with variation in the relative humidity. In this figure, the polarization curve with different relative humidity on the cathode side (CRH) is illustrated. According to the figure, the best performance occurs at about 70% (Yan et al., 2006).

For a good concentration of  $O_2$  in the air through the entire FC,  $\lambda$  should be bigger than 4. The rate of air stoichiometric flow influences both the availability of  $O_2$  as well as the humidity of the membrane. A low rate limits the availability of  $O_2$  because the air is depleted of  $O_2$  when it reaches the end of the airflow channels. Also, a very high rate can dry out the membrane.

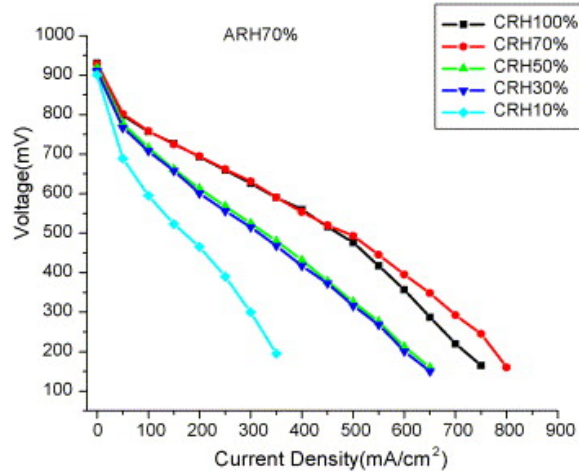


Figure 2. Polarization curves as function of feed gas humidity fuel cell (25 cm<sup>2</sup> fuel cell with triple-serpentine flow pattern, hydrogen stoichiometry = 1.2, air stoichiometry = 2). (Yan et al., 2006)

When the temperature increases, the reaction air has a drying effect and reduces the relative humidity. Low relative humidity can produce a catastrophic effect on the polymer electrolyte membrane, which not only totally relies upon high water content, but also is very thin (and thus prone to rapid drying out). The drying of the membrane changes its resistance to proton flow ( $R_M$ ).  $R_M$  is affected by the adjustment of  $\psi$ , which varies according to the following empirical equation:

$$\psi_{(k)} = \frac{\psi_{(0)}}{\left(\frac{const_2}{RH_{out(k)}}\right)^{1.12}} \quad (9)$$

where,  $\psi_{(0)}$  is the value at the saturated condition,  $RH_{out(k)}$  is the relative humidity of the outlet air at instant  $k$ , and  $const_2$  is a constant defining when the membrane is led to drying. Also, in (Fouquet et al., 2006), the variation of the resistances was associated to fault detection of flooding and drying.

Figure 3 illustrates an experimental test of the variation of  $R_M$  with different levels of relative humidity (Yan et al., 2006).

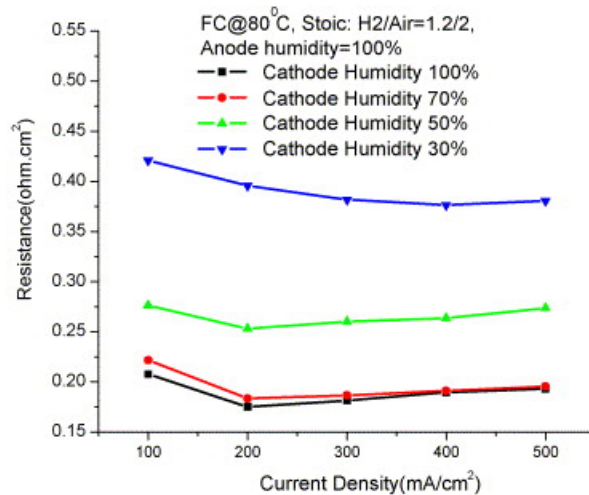


Figure 3. Fuel cell internal resistances at different feed gas humidity, anode relative humidity = 100%, (25 cm<sup>2</sup> fuel cell with triple-serpentine flow pattern, hydrogen stoichiometry = 1.2, air stoichiometry = 2). (Yan et al., 2006)

To prevent the membrane from drying, some researchers (for example (Larminie and Dicks, 2003)) proposed extra humidification in the input air. However, the variation in the relative humidity of the input air produces a very small adjustment in the output relative humidity; for example, a variation of 10% in the input relative humidity represents a variation of approximately 2% in the output relative humidity. Thus, in many cases, the extra humidification of the input air is not enough to resolve the drying problem. Figure 4 illustrates the variation on the output relative humidity produced by the adjustment in the input relative humidity.

On the other hand, a great accumulation of water causes the flooding of electrodes, making gas diffusion difficult and affecting the performance of the FC. These effects are simulated by the following equation, which was obtained empirically.

$$Rc_{(k)} = Rc_{(0)} \cdot \left( \frac{w_{acum(k)}}{const_1} \right)^{0.8}, \quad J_{max(k)} = \frac{J_{max(0)}}{\left( \frac{w_{acum(k)}}{const_1} \right)^{1.2}} \quad (10)$$

where:  $J_{max(0)}$  is the value of the maximum electrical current density at the initial state (normal condition),  $Rc_{(0)}$  is the value of the variable at the initial state (normal condition),  $w_{acum(k)}$  is the volume of water accumulated at instant  $k$ , and  $const_1$  is a constant defining when the electrodes are led to flooding.

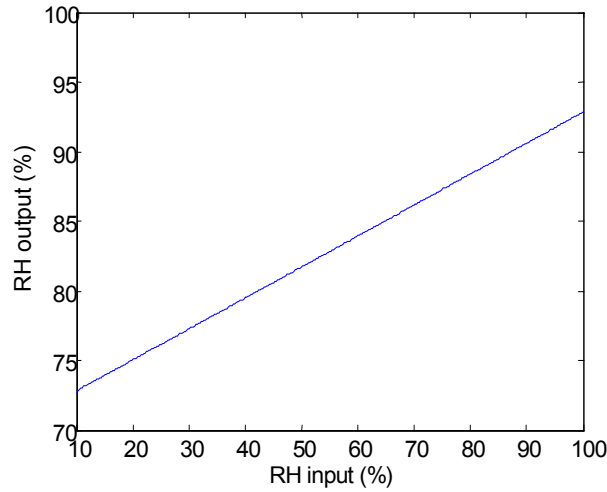


Figure 4. Variation of output relative humidity ( $RH_{output}$ ) vs. input relative humidity ( $RH_{input}$ ).

### 3. THE CONTROL TECHNIQUE

As a conclusion from the previous discussion, the ideal operational condition is relative humidity under saturated conditions. Therefore, the proposed control system adjusts the air-reaction volume to maintain the relative humidity constant.

Applying Eq. (11), the air volume for the chemical reaction (L/s) is calculated (Larminie and Dicks, 2003).

$$Flow = 3.0238 \times 10^{-4} \cdot I_{FC-adj} \cdot nr \cdot \lambda \quad (11)$$

The electrical current ( $I_{FC}$ ) was adjusted to consider internal loss current and fuel crossover ( $J_n$ ). In general,  $I_{FC-adj} = I_{FC-real} + J_n \cdot A$ .  $I_{FC-real}$  depends on the requested load, and  $nr$ ,  $A$  and  $J_n$  are constructive parameters (see Table 1). Therefore, adjusting  $\lambda$ , the regulation in the flow is performed, as shown in Eq. (12).

$$\lambda = \frac{42,1 \cdot P_{air}}{RH_{des} \cdot P_{sat\_out} - P_{w_{in}}} - 0.188 \quad (12)$$

where:  $P_{air}$  is the air pressure,  $RH_{des}$  is the desired relative humidity,  $P_{sat\_out}$  is the saturated vapor pressure in the output air,  $P_{w_{in}}$  is the partial pressure of the water in the inlet air-reaction.

The  $P_{sat}$  is calculated from the equation below:

$$P_{sat} = T^a \cdot \exp\left(\frac{b}{T} + c\right)$$

If  $T > 273.15$  K, then  $a=-4.9283$ ;  $b=-6763.28$ ;  $c=54.22$ ;

In practical applications, the air supplies the oxygen, where it has a constant pressure. In the tests, air compressor and humidifier system are not considered. Then the air is considered with pressure of 1 (atm) and at environmental temperature and humidity (25°C and 40%, respectively).

$P_{Win}$  is the partial pressure of water in the inlet air,

$$P_{Win} = P_{sat\_in} \cdot RH_{in}$$

where,  $RH_{in}$  is the relative humidity of the inlet air.

Figure 5 illustrates the block diagram of the controller developed in LabView®. The inputs of the controller are:  $J_n$ ,  $area$ ,  $I_{FC-real}$ ,  $T_{in}$ ,  $RH_{in}$ ,  $voltage$ , and  $T_{out}$ . Inside the  $F_{Air}$  block, Eq. (12) and Eq. (11) are applied to calculate the air reaction flow. Inside the  $P_{FAN}$  block (power of the refrigeration fan) an empirical equation was applied to calculate the air for refrigeration,  $P_{fan-Ref}$  depends on the requested power and  $T_{out}$ . The power is adjusted by the adjustment of  $I_{FC}$ , power-adjusted is the  $voltage$  multiplied by  $I_{FC-adj}$ .

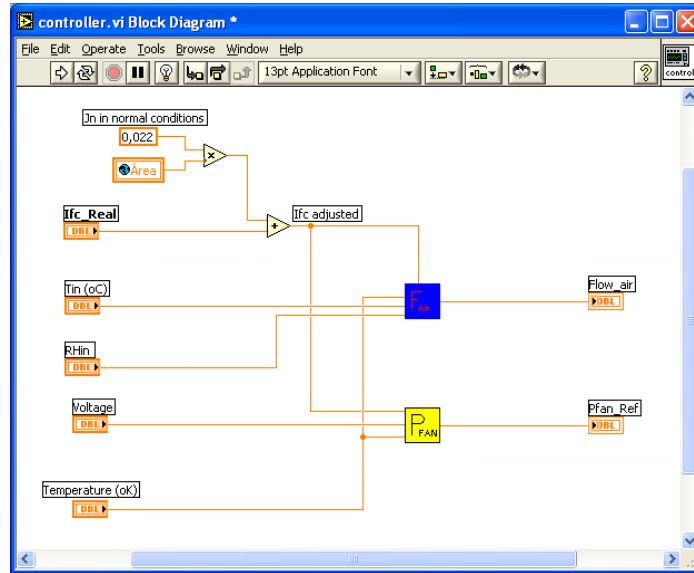


Figure 5. Controller block diagram in LabView®.

Before experimental tests, a model in Matlab® was developed. Figure 6 illustrates the evolution of the main PEMFC variables as a function of time. The variables are:  $voltage_{stack}$  (V), electrical  $current I_{FC}$  (A),  $temperature$  (°C), volume of  $airflow$  (L/min), generated heat (W), stoichiometry  $\lambda$ ,  $power$  (W) and relative humidity. From the mathematical model, the evolutions of some variables that can be difficult to monitor in a real machine (such as stoichiometry and heat) are observed. Also, predictions about the evolution of those variables can be tested, optimizing time and resources.

Initially in this test, the FC supports a constant-load demand; thus, the  $voltage$  and  $current$  should vary by themselves to maintain this demand, (i.e. the  $output$  power would be constant). And the control system regulates the air-reaction volume to maintain the relative humidity constant. The simulation begins with the FC system in stand-by (i.e. without load, and at environmental temperature, approx. 25°C). After the load requirement, the electrical equilibrium (e.g. the equilibrium of  $voltage$  and  $current$ ) is reached in less than 3 seconds. On the other hand, the temperature increases slowly as a consequence of a high inertia of the thermo-dynamical state.

At  $t=30$  minutes the thermo-dynamical state is almost stable, then step-variations of load are performed at  $t=30$  and  $t=45$  minutes to analyze the transient response; in these cases,  $voltage$  and  $electrical$  current are self-adjusted according to the requested load, the  $airflow$  volume is regulated by the control system and the  $RH_{out}$  is maintained constant (85%). Tests were conducted maintaining  $RH_{out}=85\%$  because the sensor available for experimental validation becomes inaccurate when the relative humidity is close to or is greater than 100%.

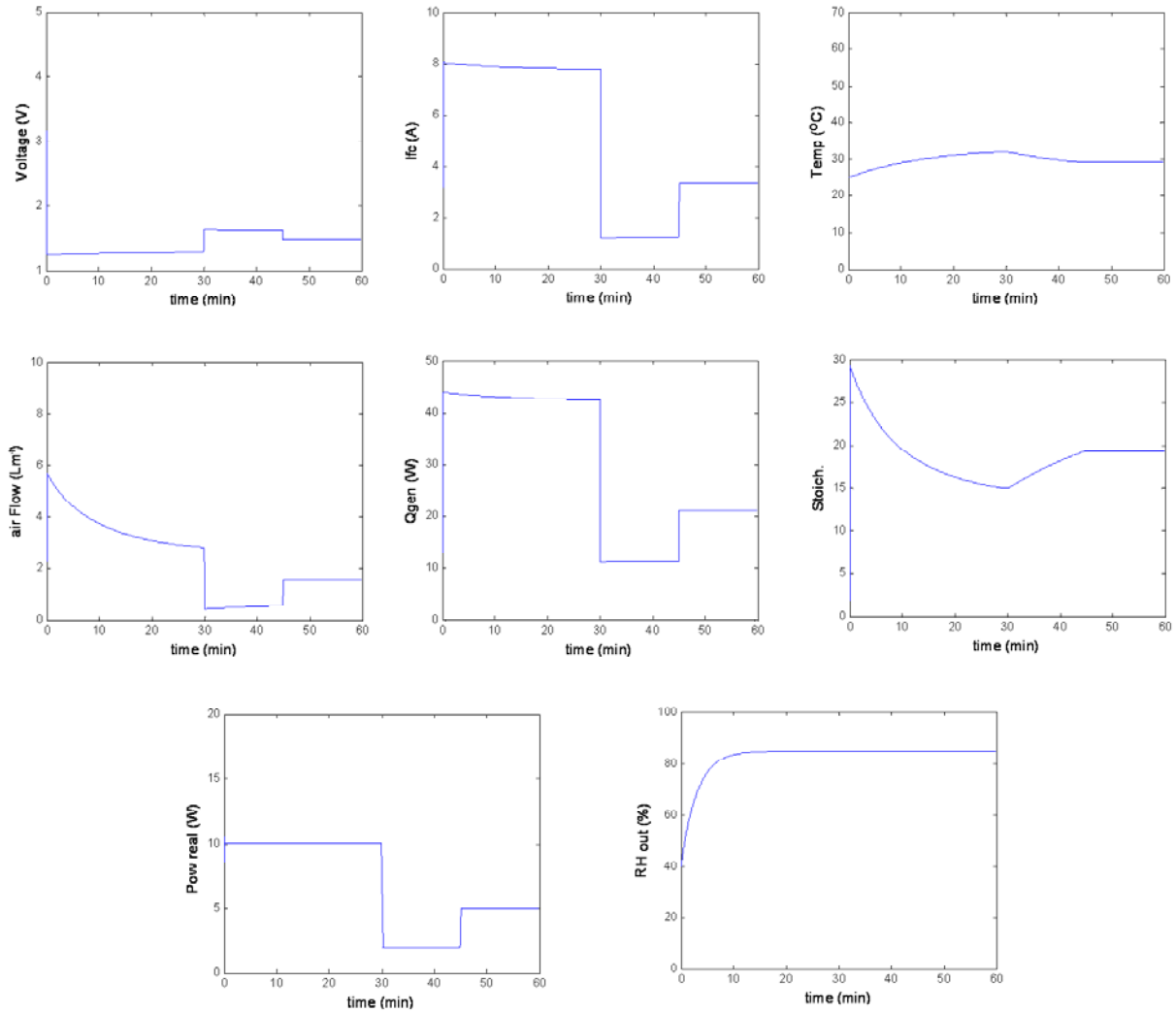


Figure 6. Operation of the FC system applying MatLab®.

#### 4. EXPERIMENTAL VALIDATION

Key issues modeling PEMFC systems are still under development; those include: lack of measurement techniques, especially real time (in situ) and non-intrusive techniques. More work is required in the areas of modeling, measurement methods and FC design optimization (Yan et al., 2006).

A fault tolerant fuel cell (FTFC) was constructed at the PSERC laboratory of the CSM (Colorado School of Mines) (Riascos, 2005) and (Riascos et al., 2006). A FTFC is a fuel cell system that permits the control and the monitoring of variables in different operating conditions, including fault conditions. The control system, the sensor system, and the power system compose the FTFC. The control system regulates the speed of the air-reaction blower and the refrigeration blower. The sensor system performs the monitoring of *voltage* ( $V_S$ ), electric *current* ( $I_{FC}$ ), temperatures ( $T_{out}$  and  $T_{in}$ ), and relative humidity ( $RH_{out}$  and  $RH_{in}$ ). The power system is composed by one AvistaLabs® cartridge containing four proton exchange membranes (PEM). A PC using the LabView® executes the control of the FTFC. The same LabView® is applied for monitoring the variables and for controlling the speed of the blowers. The reaction air and the refrigeration air are separated in different routes, which simplify the monitoring process of different variables. In this FTFC, the air for reaction is provided by a brushless DC axial blower, nominal feed 12 VDC, maximum air flow 3 CFM (cubic feet per minute), operating voltage 5 - 13.8 VDC, maximum power 0.7 W, maximum speed 4000 rpm.

Table 1. Parameters of the FTFC.

Parameter	Value
$nr$	4
$A$	$62.5 \text{ cm}^2$
$\ell$	$25 \text{ }\mu\text{m}$
$P_{O_2}$	0.2095 atm
$P_{H_2}$	1.47628 atm
$R_{C(0)}$	$0.003 \text{ }\Omega$
$B$	0.015 V
$\xi_1$	-0.948
$\xi_2$	$0,00286+0,0002.\ln A+(4,3.10^{-5}).\ln c_{H_2}$
$\xi_3$	$7.22 \times 10^{-5}$
$\xi_4$	$-1.06153 \times 10^{-4}$
$\psi_{(0)}$	23,0
$J_n$	$22 \text{ mA/cm}^2$
$J_{m\acute{a}x}$	$0.672 \text{ A /cm}^2$

Figure 7 illustrates the monitoring of the FTFC; this figure shows the FTFC, the load, and a desktop computer with the LabView® software executing the monitoring process. Table 1 presents the constructive parameters of the FTFC.

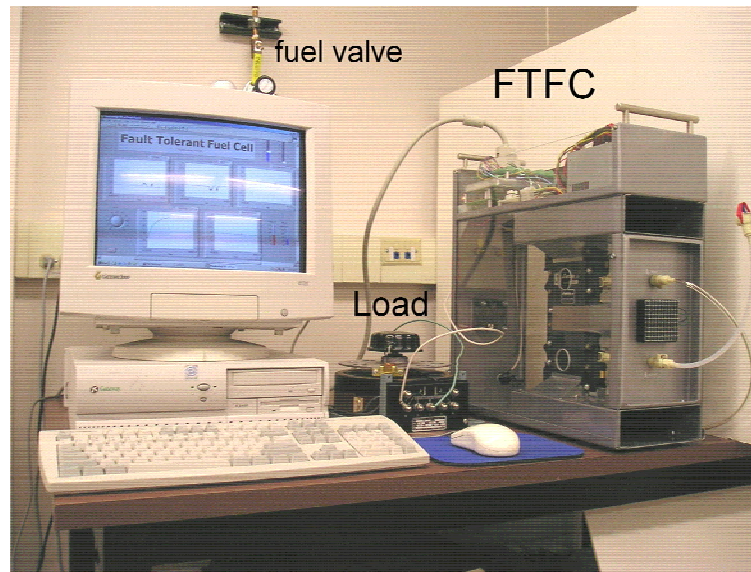


Figure 7. Monitoring the FTFC.

Figure 8 illustrates the evolution of several variables in the FTFC such as output voltage ( $V_s$ ), electric current ( $I_{FC}$ ), temperature, relative humidity ( $RH_{out}$ ), and airflow volume, under a constant load demand, using the software LabView®. The control strategy was implemented applying the same LabView®; the controller block diagram is presented in Figure 5.

An experimental test considering a temporal variation of load was conducted, in this test the load was reduced to 50% at 30 minutes, and reestablished at 45 minutes. Figure 9 illustrates the evolution of output voltage ( $V_s$ ) and electric current ( $I_{FC}$ ), and how the controller maintains a constant relative humidity ( $RH_{out}$ ).

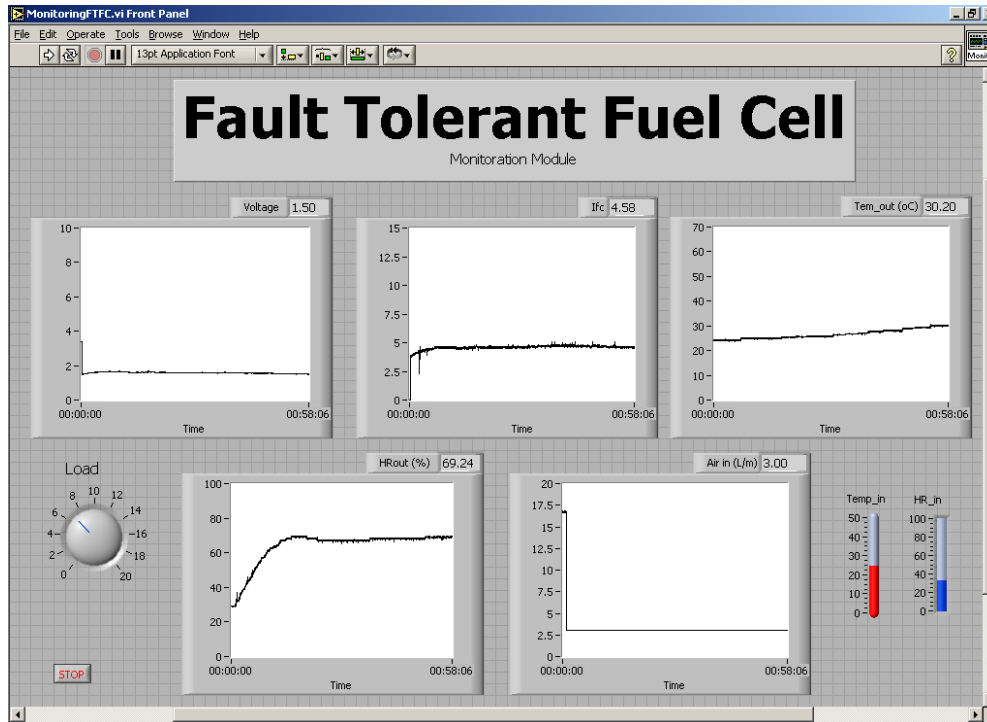


Figure 8. Monitoring the FTFC applying LabView®.

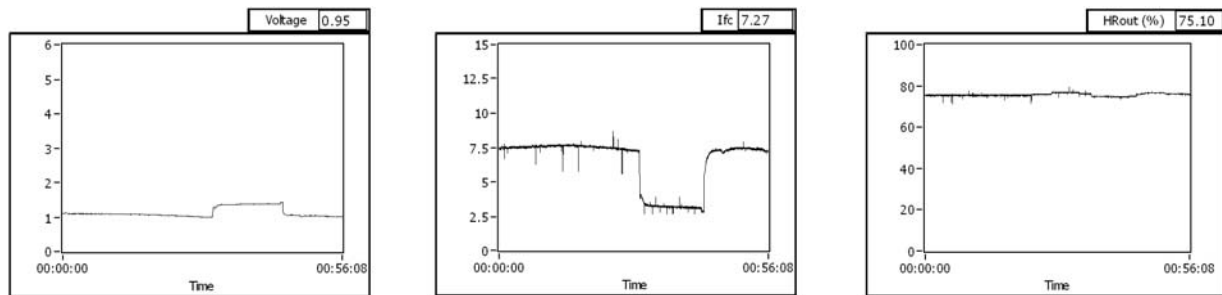


Figure 9. Evolution of the FTFC variables under different load demands.

## 5. CONCLUSIONS

The performance, stability, reliability, and cost for the current FC technology are not enough to replace internal combustion engines. A number of fundamental problems must be overcome to improve their performance and reduce costs. The control of the relative humidity is crucial to improve the performance of FC and to avoid permanent damage to the membranes.

A control technique, which maintains a constant relative humidity, was proposed. This technique regulates the rotation of the air blower adjusting the air stoichiometry and therefore regulates the relative humidity inside the FC.

A FC model was applied to analyze the evolution and to verify the dependence among the variables. From the mathematical model, the evolutions of some variables that can be difficult to monitor in a real machine are observed. Besides, predictions about the evolution of those variables can be tested, optimizing time and resources. The analysis in the FC model shows that the constant humidity control strategy is stable and consistent under different operational conditions.

Experimental tests on the Fault Tolerant Fuel Cell (FTFC) were conducted to verify the reliability of the proposed technique. In this prototype, the technique proved to be easy to implement for operating the FTFC equipment.

## 6. ACKNOWLEDGMENT

The authors thank CNPq and FAPESP for financial support.

## 7. REFERENCES

- Bao, C., Ouyanga M. and Yib, B., 2006, "Analysis of the water and thermal management in proton exchange membrane fuel cell systems", *International Journal of Hydrogen Energy* vol.31, n.8, pp. 1040-1057.
- Chang, P.A.C., St-Pierre, J., Stumper J. and Wetton, B., 2006, "Flow distribution in proton exchange membrane fuel cell stacks", *Journal of Power Sources* vol.162, n.1, pp. 340-355.
- Correa, J.M., Farret, F.A., Canha L.N. and Simoes, M.G., 2004, "An electrochemical-based fuel cell model suitable for electrical engineering automation approach", *IEEE Transactions on Industrial Electronics* vol.51, n.5, pp. 1103-1112.
- Fouquet, N., Doulet, C., Nouillant, C., Dauphin-Tanguy G. and Ould-Bouamama, B., 2006, "Model based PEM fuel cell state-of-health monitoring via AC impedance measurements", *Journal of Power Sources*, vol.159, n.2, pp. 905-913.
- Freunberger, S.A., Santis, M., Schneider, I.A., Wokaun A. and Büchi, F.N., 2006, "In-plane effects in large-scale PEMFCs," *Journal of Electrochemical Society*, vol.153, n.2, pp. A396-A405.
- Freunberger, S.A., Wokaun A. and Büchi, F.N., 2006 "In-plane effects in large-scale PEFCs", *Journal of Electrochemical Society*, vol.153, n.2, pp. A909-A913.
- Kim, G.-S., St-Pierre, J., Promislow K. and Wetton, B., 2005, "Electrical coupling in proton exchange membrane fuel cell stacks", *Journal of Power Sources*, vol.152, n.1, pp. 210-217.
- Larminie, J. and Dicks, A., 2003, "Fuel Cell Systems Explained", John Wiley & Sons Ltd.
- Promislow K. and Wetton, B., 2005, "A simple mathematical model of thermal coupling in fuel cell stacks", *Journal of Power Sources*, vol.150, n.4, pp. 129-135.
- Riascos, L.A.M., 2005, Post-doctoral research – technical report, CNPq grant nr. 201299/2003-8.
- Riascos, L.A.M.; Simoes, M.G., Cozman F.G. and Miyagi, P.E., 2006, "Bayesian network supervision on faults tolerant fuel cells", *Proceedings of the 41<sup>st</sup> IEEE-IAS (Industry Application Society)*, Tampa-FL, USA.
- Riascos, L.A.M.; Simoes M.G. and Miyagi, P.E., 2007, "Bayesian network fault diagnostic system for PEM fuel cell", *Journal of Power Sources*, vol.165, n.1, pp. 267-278.
- L.A.M. Riascos, M.G. Simoes, P.E. Miyagi, 2008, "On line fault diagnostic system for PEM fuel cell", *Journal of Power Sources*, vol.175, n.1, pp. 419–429.
- Santis, M., Freunberger, S.A., Papra, M., Wokaun A. and Büchi, F.N., 2006, "Experimental investigation of coupling phenomena in polymer electrolyte fuel cell stacks", *Journal of Power Sources* vol.161, n.2, pp. 1076-1083.
- Yan, Q., Toghianib H. and Causeya, H., 2006, "Steady state and dynamic performance of proton exchange membrane fuel cells (PEMFCs) under various operating conditions and load changes", *Journal of Power Sources*, vol.161, n.1, pp. 492-502.
- Zhan, Z., Xiao, J., Li, D., Pan M. and Yuan, R., 2006, "Effects of porosity distribution variation on the liquid water flux through gas diffusion layers of PEM fuel cells", *Journal of Power Sources* vol.160, n.2, pp. 1041–1048.